Optical and photocatalytic properties of porous TiO_2 thin films

A. BOUREZGUI[a,b,*], I. KACEM[a,b], M. KARYAOUI[a], R. CHTOUROU[a]
[a]*Laboratoire de Photovoltaïque, Centre de Recherche et des Technologies de l´énergie, BP 95 Hammam-Lif 2050, Tunisia, Faculté des sciences de Tunis El Manar, Université Tunis El Manar*
[b]*Turaif Sciences College (Northern Borders University), PO 833 Turaif 91411, KSA*

TiO_2 porous thin films were prepared using polystyrene (PS) latex particles as template in conjunction with dip coating technique. In this work, the resulting films were produced by the infiltration of the TiO_2 sol particles into the voids between the templates (templating technique). X-ray diffraction spectra (XRD) indicated that the porous TiO2/PS thin film was anatase structure. High quality of porous structures was observed by Atomic Force Microscopy (AFM) images. The transmittance spectrum has shown that elaborated thin films present a high transparency in the visible range. The photodegradation of methylene blue (MB) in the presence of TiO_2/PS thin films was performed. We found that the fabricated films exhibited better photocatalytic activity than the pure TiO_2 thin films under illumination. As a result, the porous TiO_2/PS thin film would have great potential in photocatalytic devices.

(Received February 24, 2015; accepted September 29, 2016)

Keywords: Sol gel, Dip-coating, TiO_2, Photocatalytic activity, Templating method

1. Introduction

Recently the synthesis of porous structures has attracted increasing interest of researchers as their potential applications in the field of catalysis, ion exchange, and adsorption [1]. Various strategies were taken into account regarding this sphere of study. Chiefly, templating methods include using ordered arrays of colloidal crystals [2] which seem efficient, economical and manageable, meanwhile could fit for large-scale production. Subsequent to the first successful preparation of ordered mesoporous silica [3], a significant progress has been made in the synthesis of ordered microporous (pore size below 2 nm), mesoporous (2–50 nm) and macroporous (beyond 50 nm) materials [4,5,6] and [7]. The ordered mesoporous materials are the result of using surfactants or amphiphilic block co-polymers as structure-directing agents [8], in addition, latex spheres can be used as templates to form ordered macroporous materials [9,10]. From among–very interesting thin film materials processed in this way, we list; Titanium dioxide (TiO_2) films [11]. TiO_2 has attracted considerable attention [12] due to its strong photocatalytic activity, robust chemical stability under acidic and oxidative environments, high electrical and optical properties, low production cost and non-toxicity. It has been used in numerous industrial applications such as, photocatalysis [13], optoelectronics, dye-sensitized solar cells [14], biomedical devices [15], gas sensor [16], water purification [17] etc. Many research groups have come forward with different synthetic routes to prepare porous TiO_2 thin films using a wet chemical route like hydrothermal, reverse micelle, anodization technique and sol-gel method. From among them, sol–gel method [18] seems to be the most appealing as it offers the advantage of macroporous thin film preparation at a comparatively low-cost. The combination of template and sol–gel methods has the following advantages: i) the simple preparation and size-tailoring, ii) the homogeneity of sol–gel products with high isotropy of physical, morphological and chemical properties, thus allowing the production of ordered porous TiO_2 thin films in a single-step.

In the present work, ordered TiO_2 porous thin films were prepared by sol–gel dip-coating technique. We used polystyrene (PS) latex spheres of 100 nm diameters as templates. The latex sphere templates were subsequently removed by calcination. The resulting films appear to have a high specific surface area, which will be confirmed by photocatalytic test.

2. Materials and methods

2.1. Preparation of TiO_2 sol

TiO_2 thin films were prepared using sol-gel dip-coating technique onto ITO coated glass or Silicon substrates [19]. In order to obtain a stable sol-solution, we used, as catalyst solvent, twelve moles of methanol (CH_3OH), four moles of isopropanol (CH_3CH (OH)–CH_3), four moles of acetic acid (CH_3COOH) and one mole of titanium isopropoxide $Ti(OCH(CH_3)_2)_4$ as precursor. The obtained mixture was continuously stirred for 2 h at room temperature.

2.2. Preparation of porous TiO_2 thin films

Before using, glass and silicon substrates were ultrasonically cleaned during 15 min with respectively acetone and isopropanol then rinsed with deionized water and finally dried in air at room temperature. The latex solution of the polystyrene template was prepared at concentration of 0.3% by diluting the polystyrene latex solution with deionized water. Then, the polystyrene spheres were dispersed ultrasonically in the solution. The PS spheres were assembled onto clean ITO glass substrates by dip-drawing method [20]. After completely drying the suspension, the PS colloidal crystal template was formed on the two sides of the substrate. Then, the polystyrene film was thermoset at 90 °C for 2 h to enhance the bonding among PS microspheres. Dip-coating technique was used to fill TiO_2 sol onto the PS templates. The PS array templates onto substrates were lowered into the coating solution and then withdrawn at a regulated speed of 0.6 cm s^{-1}. TiO_2 sol particles filled the voids between the template microspheres. After each coating, the films were first dried at 100 °C for 15 min. The films were then heat-treated at different temperatures ranging from 400 to 700 °C with increasing temperature rate of 5 °C min^{-1} for 2 h in furnace and used for characterizations.

3. Results and discussion

X-ray diffraction (XRD) spectra were recorded with an automated Bruker D8 advance X-ray diffractometer with CuK radiations (40 kV and 30 mA) for 2θ values over 15 – 45°. The (XRD) patterns of the TiO_2 thin films templated by PS spheres and deposited on silicon substrates at different annealing temperatures for 2 hours are shown in Fig. 1. At 350°C, the TiO_2 thin film XRD has shown no crystalline phase corresponding to the amorphous phase of TiO_2. After 400°C, PS spheres disappeared keeping a voids network. Increasing the annealing temperature to 550°C, as shown in Fig. 1, two diffraction peaks located at 2θ = 25.5° and 2θ = 38 ° are found, which belong to anatase (101) and (004) peaks, respectively [21]. We also note that the peaks intensity of the anatase phase increase with the annealing temperature. This behavior is due to the enhancement of Ti-O bonding of crystalline phase formation and leads to an increase of the crystallites size at higher temperature. The PS templates method used in this work did not change the crystalline properties of TiO_2 thin films. In addition, it has enhanced the specific surface area of thin films, which was confirmed by AFM observations.

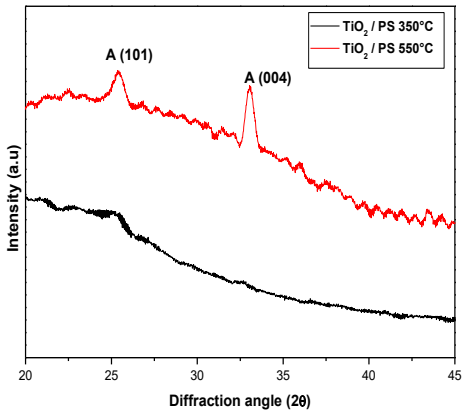

Fig. 1. XRD pattern of TiO_2 thin porous films templated by PS latex spheres (d=100 nm) heat treated at 350 °C and 550°C. A = anatase

The FTIR spectra were obtained with a Fourier transform infrared spectrometer (genesis II DTGS). The scanning wavelength of infrared was 4000 – 400 cm^{-1}. Fig. 2 shows the FTIR spectra recorded in the wavelength range 400-1800 cm^{-1} for the TiO_2 films, deposited on silicon substrates at 450, 500, and 550 °C respectively. The spectrum shows a band around 438 cm^{-1}, which is assigned to the Ti–O–Ti stretching vibration in the anatase phase [22]. These results are in conformity with the XRD results obtained above.

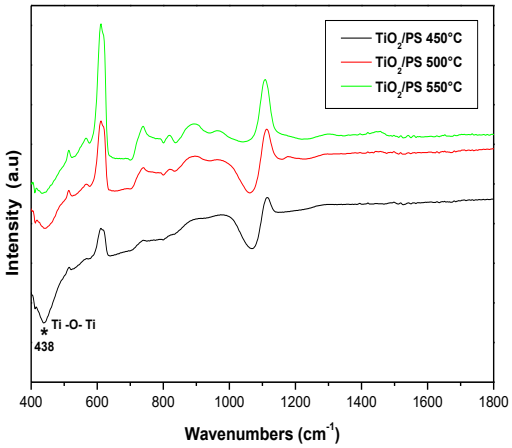

Fig. 2. FT-IR spectrum of TiO_2 thin porous films templated by PS latex spheres (d=100 nm) heat treated at 450 °C, 500°C and 550°C

The surface microstructure and roughness of samples were analyzed using an atomic force microscope, AFM, (Nanoscope 3100 Digital instrument in the tapping mode). The size, film thickness and roughness were found with WSxM software ver.5.0 [23]. Fig. 3 shows the surface morphology of TiO_2/PS films annealed at 350°C, 450°C and 550°C respectively. At 350°C, AFM images indicate that the PS spheres were not yet disappeared. At 450°C, the shape of PS particles was almost destroyed keeping an ordered porous structure. The ordered pore arrays had a

pore diameter of about 90 nm. The TiO_2 films root mean square (RMS) roughness is decreased from 4.48 to 1.38 nm and we have assigned this behavior to the removal of PS spheres. RMS roughness and thickness increase respectively from 1.38 to 2.14 nm and from 4.5 to 7 µm when the annealing temperature increases from 450 to 550°C. The increase of roughness and thickness can be interpreted as the phase change.

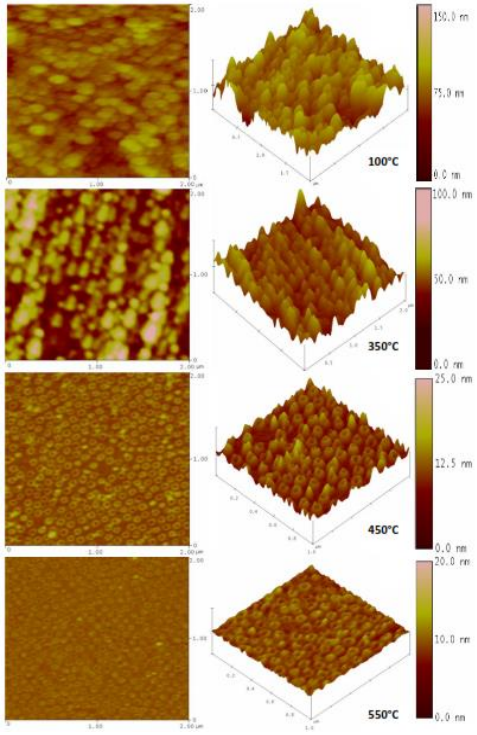

Fig. 3. AFM surface morphology images of TiO_2/PS thin porous films corresponding to the annealing temperatures of 100°C, 350°C, 450°C and 550°C

The optical Transmittance properties of the films were examined using a (UV-VIS-NIR) Perkin Elmer Lambda 950 spectrophotometer in the wavelength range of 300-1500 nm at room temperature. The transmittance T, is provided by the Beer-Lambert Law as the ratio of the transmitted light intensity to the incident light intensity [24]:

$$T = I / I_0 \quad (1)$$

Where I_0 represents the intensity of incident light and I represents the intensity of transmitted light. Fig. 4 shows the transmittance (T) spectra of the TiO_2 porous thin films deposited on Silicon substrates and annealed at different temperatures ranging from 450°C to 550°C in wavelength range between 300 and 900 nm. It can be seen from this figure that all samples present a high transparency in the visible region (400- 800 nm). This behaviour is due to the wide band gap of TiO_2 films (Eg = 3.2 eV) [25]. Moreover, the maximum of transmittance of these films decreases with increasing temperature. This phenomenon could be due to an increase in the interface scattering. From Fig. 4, we can also note that the transmittance spectrum of all films shows a low transmittance (strong absorption) in ultraviolet region with spectral wavelength between 300 and 400 nm exhibiting typical transmittance spectra of TiO_2 films [26, 27]. Fig. 4 shows also that with increasing temperature, the porous films exhibit a small red-shift compared to the pure TiO_2. This phenomenon confirms the best efficiency of temperature on the ultraviolet light absorption of ordered TiO_2 porous films.

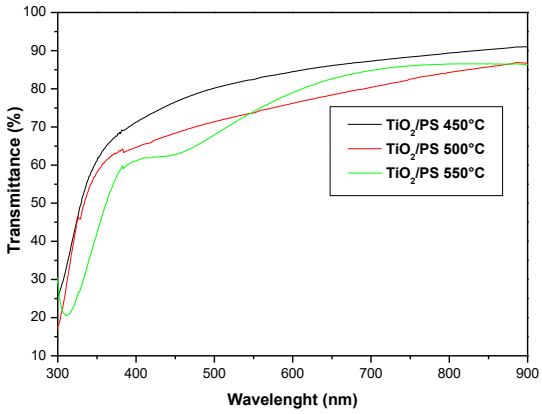

Fig. 4. Optical transmittance spectra of TiO_2/PS thin porous films as a function of annealing temperature

The photocatalytic activity of the films was evaluated by the photodegradation of (MB) in aqueous solution under UV irradiation. The UV light was obtained using a lamp (Northen Electronic. Wigan. Lancs). Typically, 25 mL of methylene blue aqueous solution (3 mg L^{-1}) was placed in a box and photocatalyst films (area of 2×2 cm^2) were placed into the solution for each test (Fig. 5). Prior to irradiation, the solution was magnetically stirred in the dark for 30 min to establish an adsorption-desorption equilibrium among the photocatalysts, MB and atmospheric oxygen. In this study, we did a quick test (30 minutes) of photocatalytic activity of both pure TiO_2 and porous TiO_2/PS photocatalysts. UV–visible absorption spectrum, recorded on the methylene blue aqueous solution before and after contact with both photocatalysts, is given in Fig. 5. The concentration variation of (MB) was evaluated by measuring the absorbance intensity using Carry UV-Visible absorption spectroscopy. The absorbance A, is provided by the Beer-Lambert Law as the logarithm of the ratio of the incident light intensity to the transmitted light intensity [24]:

$$A = \ln (I_0 / I) \quad (2)$$

Where, I_0 represents the intensity of incident light and I represents intensity of transmitted light. For all samples, calcined at 550°C, the most observed peak is at 660 nm (λ_{max} for MB) which is attributed to its monomer [28,29].

As illustrated in this figure, TiO_2/PS sample presents higher intrinsic activity for the photodegradation of (MB) than the only TiO_2. This activity is demonstrated by the considerable decrease in the absorbance, which is related to the decrease of (MB) concentration in the solution. The superior photocatalytic activity of the TiO_2/PS film can be explained by the ordered porous structure, high crystallinity of anatase phase [30] and enhancement of the specific surface [31]. In fact, the ordered porous structure with high specific surface area can offer more active adsorption sites and photocatalytic reaction centers. This phenomenon can be explained by the fact that the active sites are usually located in the pores and a high specific surface area means a high adsorptive capacity [32]. These conclusions were in agreement with results reported previously by several authors and recently by our research group [19]. In fact, Ruey-an Doong et al [20] have studied the photodegradation of (MB) by porous TiO_2 films in aqueous solution under UV irradiation. They have demonstrated that the photodegradation efficiency of MB by TiO_2 porous films was higher than that pure TiO_2.

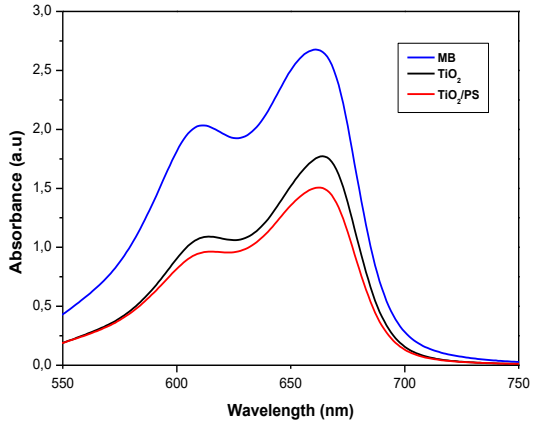

Fig. 5. Variation of the dye absorption spectra for TiO_2 thin porous films elaborated with and without PS templated spheres on the photocatalytic activity

4. Conclusion

In this study, a porous TiO_2/PS thin film was successfully prepared by sol gel dip-coating technique using PS templates method. X-ray diffraction and IR spectra show that thin films obtained crystallize into tetragonal anatase phase. Atomic Force Microscopy (AFM) images show that these films have an ordered porous structure. The analysis of the UV–Vis transmittance spectra shows that TiO_2/PS thin films are transparent in the visible range and opaque in the UV region. In comparison with TiO_2 thin films (prepared without templating method), the TiO_2/PS thin films exhibited better photocatalytic activity in the photodegradation of (MB). This enhancement can be correlated with the high specific surface area which means a high adsorptive capacity. These results illustrate the potential of the TiO_2 porous films as an effective material which can be widely applied in the field of photocatalysis to purify water and wastewater

References

[1] Zaiku Xie, Zhicheng Liu, Yangdong Wang, Qihua Yang, Longya Xu, Weiping Ding, in International Journal of Molecular Sciences **11**, 2152 (2010).
[2] Marcus Liew Kai Hoa, Meihua Lu, Yong Zhang, Advances in Colloid and Interface Science **121**(1–3), 9 (2006).
[3] C. T. Kresge, M. E. Leonowicz, W. J. Roth, J. C. Vartuli, J. S. Beck, Nature **359**, 710 (1992).
[4] Markus Reichinger, Wolfgang Schmidt, Vaishali V. Narkhede, Weiping Zhang, Hermann Gies, Wolfgang Grünert, Microporous and Mesoporous Materials **164**(0), 21 (2012).
[5] Johan A. Martens, Jasper Jammaer, Sneha Bajpe, Alexander Aerts, Yannick Lorgouilloux, Christine E. A. Kirschhock, Microporous and Mesoporous Materials **140**(1–3), 2 (2011).
[6] Shriya K. Seshadri, Hatem M. Alsyouri, Y. S. Lin, Microporous and Mesoporous Materials **129**(1–2), 228 (2010).
[7] M. Enterría, F. Suárez-García, A. Martínez-Alonso, J. M. D. Tascón, Microporous and Mesoporous Materials **151**(0), 390 (2012).
[8] D. Zhao, J. Feng, Q. Huo, N. Melosh, G. H. Fredrickson, B. F. Chmelka, G. D. Stucky, Science **279**, 548 (1998).
[9] Young Gun Ko, Dong Hun Shin, Gil Sun Lee, Ung Su Choi, Colloids and Surfaces A: Physicochemical and Engineering Aspects **385**(1–3), 188 (2011).
[10] Zhiqiang Sun, Yunfeng Li, Yanfang Wang, Xin Chen, Junhu Zhang, Kai Zhang, Zifeng Wang, Chunxiao Bao, Jianbo Zeng, Bing Zhao, Bai Yang, Langmuir **23**(21), 10725 (2007).
[11] Tahar Touam, Mohamed Atoui, Ilhem Hadjoub, Azeddine Chelouche, Boubekeur Boudine, Alexis Fischer, Azzedine Boudrioua, Abdellaziz Doghmane, Eur. Phys. J. Appl. Phys. **67**, 30302 (2014).
[12] Y. F. You et al., Ceram. Int **40**, 8659 (2014).
[13] S. Malato, P. F. Ibáñez, M. I. Maldonado, Catal. Today **147**, 1 (2009).
[14] M. A. Ehsan et al., Journal of Solid State Chemistry **230**, 155 (2015).
[15] J. Y. Jiang et al., Applied Surface Science **347**, 591 (2015).
[16] X. Li et al., Sensors and Actuators B: Chemical **219**, 158 (2015).
[17] G. Em. Romanos et al., Journal of Hazardous Materials **211**, 304 (2012).
[18] A. Choodum et al., Sensors and Actuators B: Chemical **215**, 553 (2015).
[19] J. Ben Naceur et al., Curr. Appl. Phys. **12**, 422 (2012).
[20] R. Doong et al., Separation and Purification Technology **58**, 192 (2007).

[21] Orendorz et al., Surface Science **600**(18), 4347 (2006).
[22] V. G. Erkov, S. F. Devyatova, E. L. Molodstova, T. V. Malsteva, U. A. Yanovskii, Appl. Surf. Sci. **166**, 51 (2000).
[23] I. Horcas et al., Rev. Sci. Instrum. **78**, 013705 (2007).
[24] J. M. Parnis, K. B. Oldham, Journal of Photochemistry and Photobiology A: Chemistry **267**, 6 (2013).
[25] I. Ben Assaker et al., Applied Surface Science **351**, 927 (2015).
[26] Y. H. Peng, G. F. Huang, W. Q. Huang, Adv. Power Technol. **23**, 8 (2012).
[27] C. Li et al., Thin Solid Films **570**, 436 (2014).
[28] S. H. Oh, D. J. Kim, S. H. Hahn, E. J. Kim, Mater. Lett. **57**(26–27), 4151 (2003).
[29] A. K. Ghosh, P. Mukerjee, J. Am. Chem. Soc. **92**, 6408 (1970).
[30] A. Guillén-Santiago, S. A. Mayén, G. Torres-Delgado, R. Castanedo Pérez, A. Maldonado, M. de la L. Olvera. Materials Science and Engineering: B **174**(1–3), 84 (2010).
[31] Jianquan Zhao, Peng Wan, Jing Xiang, Tong Tong, Lei Dong, Zhinong Gao, Xinyu Shen, Hua Tong, Microporous and Mesoporous Materials **138**(1–3), 200 (2011).
[32] M. Karyaoui, A. Souissi, J. Ben Naceur, K. Boubaker, M. Amlouk, R. Chtourou, Trade Science Inc. Ma 792212530 (2012).

*Corresponding author: bourezgui.aymen@gmail.com